INDERSCIENCE PUBLISHERS
Linking academia, business and industry through research

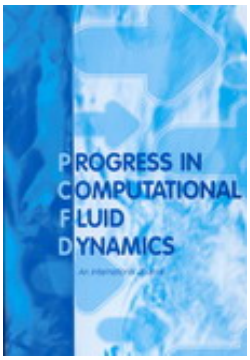

Progress in Computational Fluid Dynamics, An International Journal

ISSN online: 1741-5233 - ISSN print: 1468-4349
https://www.inderscience.com/pcfd

Investigation of kinetics of thin layer drying of fruits using computational fluid dynamics

Chukwunonso F. Nwoye, Chukwunenye Okoronkwo, Godswill Nwaji, Ezenwa N. Obiora

DOI: 10.1504/PCFD.2024.10060948

Article History:

Received:	10 February 2022
Last revised:	30 March 2023
Accepted:	30 March 2023
Published online:	20 December 2023

Investigation of kinetics of thin layer drying of fruits using computational fluid dynamics

Chukwunonso F. Nwoye*

Mechanical Engineering Department,
Akanu Ibiam Federal Polytechnic Unwana,
Afikpo, Ebonyi State, Nigeria
Email: royalpriest20@yahoo.com
*Corresponding author

Chukwunenye Okoronkwo and Godswill Nwaji

Mechanical Engineering Department,
Federal University of Technology,
Owerri, Imo State Nigeria
Email: chukwunenyeanthonyokoronkwo@gmail.com
Email: godswillmee@gmail.com

Ezenwa N. Obiora

Mechanical Engineering Department,
Nnamdi Azikiwe University,
Awka, Anambra State, Nigeria
Email: obiora.ezenwa@yahoomail.com

Abstract: The roles of temperature and velocity of air and the limits of their influence in thin layer drying of fruits were studied using computational fluid dynamics code – ANSYS FLUENT 18. Unripe banana (*Musa cavendishii*) was used as sample and mass transport from the fruit to the drying air was simulated by solving specie transport equation without reaction. Velocity helped to regulate the concentration gradient between the chamber space and the fruits surface as it was responsible for the transportation of free H_2O molecules at the surface of the fruit to the environment. Temperature on the other hand was the major determinant of the rate at which species were transported from the fruit to the drying air and it is defined by mass diffusivity. The computed values of effective diffusivity at the test temperatures ranged between 1.62E-10–3.85E-10. However, these values dropped slightly when shrinkage effect was factored in.

Keywords: drying; fruits; CFD; turbulence; porous medium; shrinkage.

Reference to this paper should be made as follows: Nwoye, C.F., Okoronkwo, C., Nwaji, G. and Obiora, E.N. (2024) 'Investigation of kinetics of thin layer drying of fruits using computational fluid dynamics', *Progress in Computational Fluid Dynamics*, Vol. 24, No. 1, pp.54–64.

Biographical notes: Chukwunonso F. Nwoye is a PhD student in Federal University of Technology Owerri and a Lecturer in the Department of Mechanical Engineering, Akanu Ibiam Federal Polytechnic Unwana, Nigeria. His research interest includes computational fluid dynamics, combustion, fluid flow analysis and renewable energy.

Chukwunenye Okoronkwo is a Professor in Mechanical Engineering Department at Federal University of Technology Owerri. He has over 15 years of teaching and research experience and majored in Energy and power systems. He has published in several reputable journals including *Journal of Energy Engineering*. One of his recent works include: transient simulation of a building integrated hybrid solar collector/nocturnal radiator with in-built thermal storage for space cooling in Owerri Nigeria. His research interests include energy policy and planning, applied energy studies, renewable energy and numerical simulation.

Godswill Nwaji obtained his PhD in Mechanical Engineering from Federal University of Technology Owerri where he currently lectures. His research focus include; renewable energy, heat transfer and numerical simulation. He has published in reputable national and international journals and conferences.

Ezenwa N. Obiora obtained his Master's in Mechanical Engineering from Nnamdi Azikiwe University Awka, Nigeria were he currently lectures. He has over ten years of teaching and research experience and majored in thermal engineering. He has published in several reputable journals and his recent works include; Development of Ceiling Board using Breadfruit Seed Coat and Recycled Low Density Polyethylene published in Heliyon and Trend appraisal of Nigeria's energy sector and its implication on living standards published in *International Journal of Energy Technology and Policy*. His current research interest includes energy conversion, numerical simulation, energy policy and planning and material development.

1 Introduction

Most countries are endowed with resources to meet its own food need from domestic production (Clapp, 2015). What obtains however, especially in developing countries is that food availability is seasonal; usually in overwhelming abundance and very cheap during harvest and in short supply and almost unaffordable shortly after. Low-cost of product during harvest is partly due to the forces of demand and supply and the need for the farmer to quickly dispose of the goods to cut losses that can arise from spoilage. Some of the consequences of this are food shortage, low income for the farmer and loss of financial resources that would have helped stimulate the economy to other countries should importation becomes an option.

To guarantee constant food supply and good reward for the farmer, attention must be paid to food processing and preservation. Some food preservation techniques include drying, canning, pickling, freezing, etc. The technique of interest here is drying. This is due to its low energy and technical requirement and ease of set up compared to canning and freezing.

Drying is a post-harvest processing operation that removes water from food products in order to reduce microbial activities and increase shelf life. Food water content vary with class. In fruits and vegetables for example, the range is between 90%–98% (Derossi et al., 2011) and 13%–20% in grains (Kenneth and Hellevang, 1995). Above 10%, water in food encourages microbial activities which leads to degradation and spoilage (Camelia et al., 2008). In addition to preservation, drying also reduces the physical size, mass, transportation cost and packaging requirement of products (Onwude et al., 2016; Jaruk and Roberts, 2007).

Several techniques are available for drying, some of which include air drying, microwave drying, osmotic dehydration, infrared drying and ultrasonic drying (Derossi et al., 2011). Of all these, air drying is the most common. In air drying, heat is transferred from the surrounding air to the food material. This increases the energy of the water molecules at the surface of the food causing them to evaporate. At the same time, water molecules from within negotiates its way to the surface to replace the evaporated ones. This water transport from the interior to the surface happens through mechanisms such as capillary flow, diffusion, water evaporation and condensation (Camelia et al., 2008; Onwude et al., 2016).

Air drying can therefore be effectively divided into two phases; the transfer of water molecules from the food surface to the surrounding air by evaporation and transportation of water from within the food to the surface both of which occur simultaneously. The evolution of these phases determine the rate at which products dry and they are influenced by mass, momentum and energy conservation, and specie transport.

The plot of moisture content with respect to drying time often known as the drying curve is used to show drying trend or drying behaviour of products (Sabarez, 1998). Drying curve (Figure 1) is an exponential curve and generally divided into an initial constant rate period, and one or more falling rate period (Onwude et al., 2016).

Figure 1 Drying curve of agricultural products

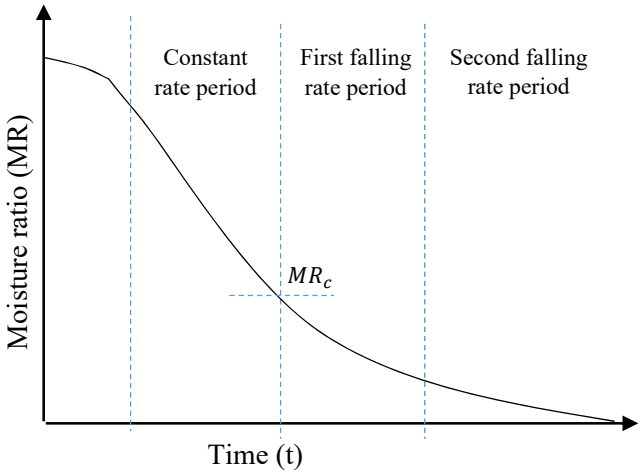

Source: Onwude et al. (2016)

For some products such as pumpkin, carrot and kiwi the drying curve show both constant and falling rate periods (Onwude et al., 2016). However, the drying curve for majority of fruits and vegetable products, are characterised by only falling rate period (Lutovska et al., 2015) and (Onwude et al., 2016). The crucial information conveyed by the curve is the mechanism that dominate the drying process. While the constant rate period is largely controlled by capillary forces and gravity and subject to external factors like temperature, velocity and humidity (Onwude et al., 2016), the falling rate period is dominated by diffusion and controlled by both external and internal variables like shape, size, microstructure and the chemical properties of the food which affect its affinity for water (Derossi et al., 2011).

Products with high moisture content often show constant rate period. The evaporation of water molecules from the

surface of the product and its transport from the interior to the surface occurs at a uniform rate so that water concentration at the surface is kept constant. This continues until the critical moisture content (MR_c) is reached. At this stage, falling rate period begins and diffusion controls the drying process going forward. The resistance to water transport to the surface is increased due to extended tortuous path and resistance to flow occasioned by compression of cells or shrinkage (Sabarez, 1998). The surface film of the product becomes hard and dry even though the interior moisture content might still be significant. Evaporation can also occur within the food cells and diffuse to the surface due to differences in vapour pressure.

Drying air condition is defined by velocity, temperature and humidity. The values and the distribution of these variables within the drying chamber affects drying rate, energy consumption and uniformity of drying.

The aim of this work therefore is to numerically investigate the influence of velocity and temperature mix in the drying trends of fruits using unripe banana (*Musa cavendishii*) as sample.

Literatures on theories of mass transfer and drying models would be reviewed further, followed by detailed description of the methodology used in the analysis, next would be the presentation/discussion of results obtained and drawn conclusions.

1.1 Mathematical models

To achieve uniform drying, food materials are thinly sliced in such a way that they are fully exposed to air stream and arranged so that air flow and temperature over the material is uniform. This is known as thin layer drying. To achieve this, the products are set in layers on mesh trays within the drying space. Hot drying air flows over or through the food material and are usually operated in batch manner (Rajasekar et al., 2016).

During drying, water molecules diffuse from the internal region where they are in high concentration to the surface where the concentration is lower and evaporates into the unsaturated air on absorbing some heat energy from the air. Diffusion therefore, is considered as the dominant mechanism for internal moisture transfer (Lopez et al., 2015; Sabarez, 1998; Derossi et al., 2011). This transfer due to diffusion is predominantly driven by concentration gradient. Steady diffusive mass flux of species due to concentration gradient for one dimensional diffusion is given by Fick's first law as (Incropera et al., 2007);

$$m_{i,diff} = -\rho D_{i,m} \frac{\partial (m_{i,f})}{\partial x} \tag{1}$$

where $m_{i,diff}$ is the diffusive mass flux of specie i and ρ is the mixture density, $D_{i,m}$ is the diffusion coefficient and $m_{i,f}$ the mass fraction of specie i

For most drying operation, the boundaries of the food material is stationary and the diffusion flux can be represented as shown in Figure 2

The conservation of mass equation through the system can be written as

$$-\frac{\partial (m_{i,diff})}{\partial x} = \frac{\partial m_i}{\partial t} \tag{2}$$

where m_i is the mass of specie i

The right hand side of equation (2) can be written in terms of mass fraction and equation (1) can be substituted into the left hand side as

$$\frac{\partial}{\partial x}\left(\rho D_{i,m} \frac{\partial (m_{i,f})}{\partial x}\right) = \frac{\partial (\rho m_{i,f})}{\partial t} \tag{3}$$

$$D_{i,m} \frac{\partial^2 (m_{i,f})}{\partial x^2} = \frac{\partial (m_{i,f})}{\partial t} \tag{4}$$

Figure 2 Diffusion of moisture from food material to the environment (see online version for colours)

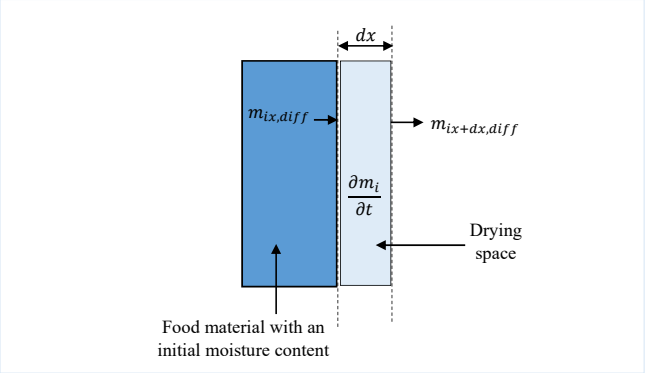

1.1.1 Crank model

The solution to equation (4) which is Fick's second law of diffusion can be achieved using numerical methods and it is a function of sample geometry. Crank in 1975 developed analytical solution to this effect. The solution represents the drying behaviour during the falling rate period for simple geometries such as slab, finite slab, cylinder, finite cylinders, sphere, etc. The solution for slab geometry is (Onwude et al., 2016).

$$\begin{aligned} MR &= \frac{M_t - M_e}{M_O - M_e} \\ &= \frac{8}{\pi^2}\frac{1}{(1)^2} exp\left(\frac{-(1)^2\pi^2 D_{e,ff} t}{4(h)^2}\right) + \frac{1}{(3)^2} exp\left(\frac{-(3)^2\pi^2 D_{e,ff} t}{4(h)^2}\right) \\ &+ \frac{1}{(5)^2} exp\left(\frac{-(5)^2\pi^2 D_{e,ff} t}{4(h)^2}\right) + \cdots \\ &+ \frac{1}{(2n+1)^2} exp\left(\frac{-(2n+1)^2\pi^2 D_{e,ff} t}{4(h)^2}\right)\Bigg] (n \in N \to +\infty) \end{aligned} \tag{5}$$

Equation (5) can be written in compact form as

$$MR = \frac{M_t - M_e}{M_O - M_e} = \frac{8}{\pi^2}\sum_{n=0}^{\infty}\frac{1}{(2n+1)^2}exp\left(\frac{-(2n+1)^2\pi^2 D_{e\,ff}\,t}{4(h)^2}\right) \quad (6)$$

For long drying period, only the first term of the series applies and equation (5) can be simplified as

$$MR = \frac{M_t - M_e}{M_O - M_e} = \frac{8}{\pi^2}exp\left(\frac{-\pi^2 D_{e\,ff}\,t}{4h^2}\right) \quad (7)$$

where h is half thickness of the slab, MR is the moisture ratio, M_t is the moisture content at time t and M_O and M_e respectively are moisture content at time zero and equilibrium. Compared to M_t and M_O, M_e is relatively small and may be neglected in the computation process. Solution to Fick's diffusion equation are generally the same for most of the geometries with variation coming from shape factors which is $\frac{8}{\pi^2}$ for slab geometry.

1.1.2 Shrinkage model

Removal of water from the pores of the food material will give rise to compression stress which causes the wall of the cell to contract. This contraction effect is known as shrinkage. Shrinkage of the cells makes it more difficult for water to be transported. Therefore, moisture diffusivity estimated without considering the effect shrinkage will always be above the practical value. This was demonstrated by Guhong et al. (2012) in convective drying of bio-porous materials and (Ramallo and Mascheroni, 2011) while modelling the effect of shrinkage on pineapple drying.

To compute effective diffusivity of slab geometry considering shrinkage equation (8) can be used (Onwude et al., 2016).

$$ln\left(\frac{Y_t}{Y_0}\right) = ln\left(\frac{8}{\pi^2}\right) - \frac{\pi^2 D_{e\,fs}\,t}{4L^2} \quad (8)$$

where L is the length of slab, D_{efs} is effective diffusivity considering shrinkage

$Y_t = M_t/V_t$, $Y_0 = M_0/V_0$,

V_0 is the initial volume of the sample and V_t the volume of sample at time t

Shrinkage (S) can be approximated to the volume of water removed (Amira et al., 2014) and written as a function of present and initial volume of the food material (Guohong et al., 2012)

$$S = 1 - V_t/V_0 \quad (9)$$

$$V_t = \frac{M_t}{\rho_t} \text{ and } \rho_t = \rho_o(1 - \in_t)$$

$\in_t$ is the porosity of the material at time t and ρ_o is the initial density of the material

1.1.3 Arrhenius law

The relationship between effective diffusion coefficient and temperature is often represented using Arrhenius type equation.

$$D_{eff} = D_o exp\left(\frac{E_a}{RT}\right) \quad (10)$$

where D_o (m^2/s)-the pre-exponential factor is a constant, E_a is the activation energy(KJ/mol), R gas constant (8.314 51 $J/(mol/K)$) and T is temperature(K)

Table 1 Thin layer models for drying of fruits and vegetables

Model name	*Model*	*Bases of formulation*
Newton/Lewis model	$MR = exp\ (-kt)$	Newton's law of cooling
Page model	$MR = exp\ (-kt^n)$	Newton's law of cooling
Modified page model (I)	$MR = exp\ [-(kt)^n]$	Newton's law of cooling
Modified page model (II)	$MR = k\ exp\ (-t/d^2)^n$	Newton's law of cooling
Henderson and Pabis	$MR = a\ exp\ (-kt)$	Fick's second law
Approximation of Diffusion	$MR = a\ exp(-kt) + (1-a)\ exp\ (-kbt)$	Fick's second law
Logarithmic	$MR = a\ exp\ (-kt) + c$	Fick's second law
Silver et.al	$MR = exp\left(-at - b\sqrt{t}\right)$	Empirical
Weibull	$MR = a - bexp\ [-(kt^n)]$	Empirical
Aghabashlo	$MR = exp - \left(\frac{k_1 t}{1 + k_0 t}\right)$	Empirical

Source: Onwude et al. (2016), Iyang and Oboh (2018), and Daniel et al. (2014)

1.1.4 Drying models

There are models of varying degree of complexity used in describing the thin layer drying behaviour of food materials. Based on their derivation, these models can be classified as theoretical, semi-theoretical and empirical. Some semi-theoretical and empirical models are presented in (Table 1) they are the most widely used because few assumptions are made in their formulation and they predict drying behaviour better (Onwude et al., 2016). Empirical models are wholly derived from experiment, they do not follow theoretical fundamentals and its parameters usually do not have physical interpretations. The semi-theoretical models on the other hand are formulated based on Newton's law of cooling and Fick's second law of diffusion. Its application may depend on variables such drying air temperature, drying air velocity, relative humidity, initial moisture content and material thickness as they only work if these parameters are in the range within which the model

was developed (Iyang and Oboh, 2018). However, the ultimate determinant of the most appropriate model to be used in describing the drying behaviour of a food material is the statistical criteria. The criteria often used in literature include R^2, *RMSE*, *SSE*, *RRMS*, *MBE*, *MPE*, *MSE*, etc. (Iyang and Oboh, 2018; Onwude et al., 2016). The closer the value of R^2 is to one the better. While for the rest, the values that tends towards zero is acceptable.

1.1.5 Computational fluid dynamics models

CFD codes have been used by several researchers for drying related investigations. Lopez et al. (2015) and Kumar et al. (2012) studied the convective heat and mass transfer process while investigating the drying behaviour of chickpea and banana respectively using COMSOL Multiphysics. Bohojlo-Wisniekwska (2015) and Kolodziejczyk et al. (2016) modelled heat and mass transfer in vegetables using ANSYS fluent. Zabski (2015) also used same to simulate the drying of wood chips.

1.1.6 Standard k-ε model

The study of drying kinetics using CFD codes involves numerical solution to flow and energy equations in the drying chamber and specie transport or diffusion equation in the porous food domain. Flow through the chamber are generally turbulent. Considering the CPU resource and time required for direct simulation of turbulence, only the effect on the mean flow properties were accounted for. The whole range of turbulence scale were modelled using standard *k–ε* model which is based on Boussinesq hypothesis. The equations for turbulence kinetic energy *k* and the turbulence dissipation *ε* respectively are Versteeg and Malalasekera (1995), and Roland and Chaouat (2022)

$$\frac{\partial(\rho k)}{\partial t}+\frac{\partial\left(\rho u_i k\right)}{\partial x_i}=\frac{\partial}{\partial x_j}\left[\left(\mu+\frac{\mu_t}{\sigma_k}\right)\frac{\partial k}{\partial x_j}\right]+G_k-\rho\varepsilon \tag{11}$$

$$\begin{aligned}&\frac{\partial(\rho\varepsilon)}{\partial}+\frac{\partial(\rho u_i\varepsilon)}{\partial x_i}\\&=\frac{\partial}{\partial x_j}\left[\left(\mu+\frac{\mu_t}{\sigma_\varepsilon}\right)\frac{\partial\varepsilon}{\partial x_j}\right]+C_{1\varepsilon}\frac{\varepsilon}{k}(G_k)-C_{2\varepsilon}\rho\frac{\varepsilon^2}{k}\end{aligned} \tag{12}$$

where

$$G_k=-\rho\overline{u_i' u_j'}\frac{\partial u_j}{\partial x_i}$$

and represents the generation of turbulence kinetic energy due to mean velocity gradient.

μ_t is turbulent viscosity which is expressed as

$$\mu_t=\rho C_\mu\frac{k^2}{\varepsilon}$$

$$C_{1\varepsilon}=1.44,\ C_{2\varepsilon}=1.92,\ C_\mu=0.09,\ \sigma_k=1.0,\ \sigma_\varepsilon=1.3$$

1.1.7 Energy equation

$$\begin{aligned}&\frac{\partial}{\partial t}(\rho E)+\frac{\partial}{\partial x_i}\left(u_i(\rho E+p)\right)\\&=\frac{\partial}{\partial x_j}\left(\left(k+\frac{c_p\mu_t}{Pr_t}\right)\frac{\partial T}{\partial x_j}+u_i\left(\tau_{ij}\right)_{eff}\right)+S_h\end{aligned} \tag{13}$$

where $\left(k+\frac{c_p\mu_t}{Pr_t}\right)$ is effective thermal conductivity, k is the thermal conductivity, c_p is specific heat capacity and Pr_t the turbulent Prandtl number which is = 0.85. *E* is the total energy and $(\tau_{ij})_{eff}$ is the deviatoric stress tensor defined as

$$\left(\tau_{ij}\right)_{eff}=\mu_{eff}\left(\frac{\partial u_i}{\partial x_j}+\frac{\partial u_j}{\partial x_i}\right)-\frac{2}{3}\left(\rho k+\mu_{eff}\frac{\partial u_k}{\partial x_k}\right)\delta_{ij} \tag{14}$$

1.1.8 Species transport equation

The convection diffusion equation is expressed as

$$\frac{\partial}{\partial t}\left(\rho Y_i\right)+\nabla.\left(\rho\vec{v}Y_i\right)=-\nabla.\vec{J}_i+S_i \tag{15}$$

S_i, Y_i and $\vec{J}_i$ respectively are the user defined source term, mass fraction and turbulence diffusion flux of specie *i*. $\vec{J}_i$ is given as;

$$\vec{J}_i=-\left(\rho D_{i,m}+\frac{\mu_t}{Sc_t}\right)\nabla Y_i-D_{T,i}\frac{\nabla T}{T} \tag{16}$$

$D_{i,\,m}$ is mass diffusion coefficient for specie *i*, $D_{T,\,i}$, is the thermal diffusion coefficient, *T* is temperature and Sc_t– the turbulent Schmidt number which is = 0.7

Sc_t can be expressed as

$$Sc_t=\frac{\mu_t}{\rho D_t}$$

where μ_t is turbulent viscosity and D_t the coefficient of mass diffusion due to turbulence.

Food materials are often modelled as porous media (Lopez et al., 2015; Camelia et al., 2008; Jaruk and Roberts, 2007). Porous media models are incorporated into standard flow equation as an additional momentum source term. The source terms are of two parts; the viscous loss term and the inertial loss term which are the first and the second term respectively in the right hand of equation (17).

$$\vec{F}=\left(\frac{\mu}{k}v_i+C_2\frac{1}{2}\rho|v|v_i\right) \tag{17}$$

k is the permeability of the porous material, C_2 is the inertial resistance factor, *μ*– the dynamic viscosity, and v the velocity vector.

For packed bed of spheres, *k* and C_2 can be computed using the Ergun equations

$$k=\frac{{D_p}^2\in^3}{150(1-\in)^2} \tag{18}$$

$$C_2 = \frac{3.5(1-\epsilon)}{D_p \epsilon^3} \tag{19}$$

D_p is the particle diameter and ϵ- the porosity defined as

$$\epsilon = \frac{V_p}{V} \tag{20}$$

V is the total volume of the porous medium and V_p– the void volume.

2 Methodology

The simulation was carried out for an unripe banana sliced and arranged in layers (Figure 3) inside a cabinet tray drier of dimension 0.6 *m* × 0.4 *m* × 0.6 *m*. In the drier, hot air (modelled as a mixture of O_2, N_2 and H_2O in vapour state) flow across the trays containing the banana slices of approximately 26 *mm* diameter and 10mm thickness each.

The computational domain comprised of two zones; the drying space and the perforated tray cabinet which held the chips in place for drying. The tray together with the chips were defined as porous media consisting of fluid and solid particles in thermal equilibrium.

Figure 3 Arrangement of the banana in the drying chamber (see online version for colours)

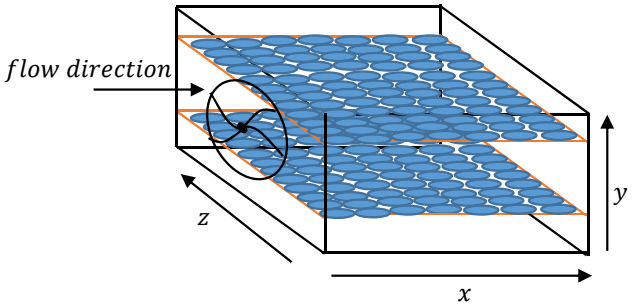

Table 2 Thermo physical properties of banana used for the simulation

Material	*Property*	*Symbol*	*Value*	*Unit*
Banana	Thermal diffusivity	α	1.8E-07	$m^2\ s^{-1}$
	Density	ρ_o	1,046	kgm^{-3}
	Thermal conductivity	K	0.894	$W.m^{-1}\ K^{-1}$
	Specific heat capacity	C_p	4,854	$J.kg^{-1}\ K^{-1}$
	Initial moisture mass fraction	$m_{w,fl}$	0.72	$kg.kg^{-1}$

Source: Rosa (2016)

At the test velocities of 0.2 *m/s*, 0.5 *m/s* and 1.0 *m/s* and length scale corresponding to air inlet opening (0.4 *m*), the Reynolds number respectively of the flow at 313 K were 4711, 11777.2 and 23554.3, hence the flow was turbulent. The whole range of turbulence scale were resolved using standard *k–ε* model with standard wall function. Moisture content of the chips was defined as water vapour to eliminate the need for multiphase model. The thermo physical and mass transfer properties of the banana used for the simulation are as shown in Table 2. The mass fraction of H_2O in the air (Table 3) were set to 0.005,0.0085 and 0.013 at the test temperatures-313 K, 323 K and 333 K respectively to keep the RH of drying air constant at 10%.

Table 3 Properties of air used for the simulation

Inlet air temperature K	$C_p\ J.kg^{-1}\ K^{-1}$	$k\ W.m^{-1}\ K^{-1}$	$\rho\ Kgm^{-3}$	$\mu\ kgm^{-1}\ s^{-1}*10^{-5}$
313	1,005.6	1.3995	1.127	1.9063
323	1,006.2	1.3991	1.093	1.953
333	1,006.9	1.3987	1.060	1.998

Inlet air temperature K	H_2O *mass fraction*	O_2 *mass fraction*	*RH %*
313	0.005	0.23	10
323	0.0085	0.23	10
333	0.013	0.23	10

The convective heat transfer coefficients h_c at the interface between the food material and drying air at the flow velocities were determined from the relationship;

$$q = h_c\,(T_w - T_m) \tag{21}$$

q was estimated by simulating the air flow between two layers of drying tray. The layers were considered as walls at constant temperature T_w whose physical and thermal properties coincided with those of the food material. T_m given by equation (22) is the area weighted average temperature in the channel at the location where q is defined.

$$T_m = \frac{\int_0^y uT(2\pi y)dy}{\int_0^y u(2\pi y)dy} = \frac{\int_0^y uTydy}{\int_0^y uydy} \tag{22}$$

Having estimated q, T_m and T_w, h_c can be computed. The plots of h_c through the length of the channel at the flow velocities were shown in Figure 4.

Lewis analogy equation (23), relate h_c to vapour transfer coefficient h_m (Miroslawa et al., 2016).

$$h_m = \frac{h_c}{\rho C_p Le^{2/3}} \tag{23}$$

ρ and C_p are the density and specific heat respectively of humid air. Le was assumed to be unity, h_m at the average values of h_c were computed and shown in Table 4.

For the purpose of computing the inertia resistance and permeability of the porous domain, the solid phase of the banana was assumed to be closely packed beds with ordered identical sphere particles of diameter (D_P) 8 μm and porosity (ϵ) 0.26. Substitution of the values of D_P and ϵ into

equation (18) and equation (19) gave the values of inertial resistance and permeability as shown in Table 5.

Table 4 Mass transfer coefficient h_m at flow velocity

Velocity m/s	h_c *w.m*$^{-2}$ *K*$^{-1}$	h_m *ms*$^{-1}$
0.2	9.19	8.3E-03
0.5	14.28	12.9E-03
1.0	17.82	16.1E-03

Figure 4 Variation of convective heat transfer with flow velocity (see online version for colours)

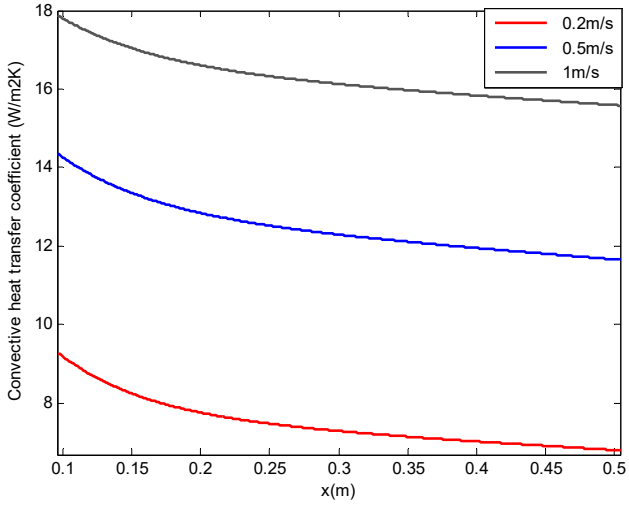

Table 5 Resistance coefficients of the porous structure

Parameter	*Symbol*	*Value*	*Unit*
Permeability	α	1.869e16	m^{-2}
Inertia resistance	C_2	2.95e8	m^{-1}

Figure 5 2D mesh profile of the flow domain (see online version for colours)

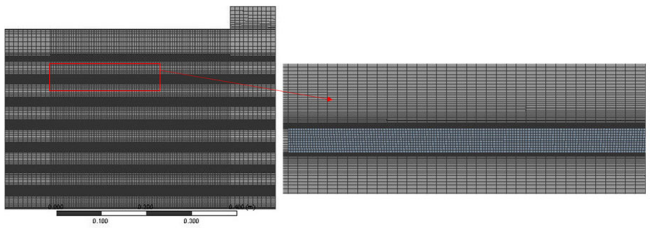

The drying space and the porous domain were mapped with 2D structured mesh of varying density (Figure 5). In the porous domain and in the space between the trays, the mesh density were relatively high. In order to capture the critical flow features effectively, more clustering was effected near the walls and at the boundaries between the trays and the drying space such that the area weighted average of the y^+ value was ~78.487.

The boundary conditions at 313 K are as specified in Table 6. At 323 K and 333K, the conditions are essentially the same except for the adjustment in the mass fraction of H_2O inlet and fruit/air interface from 0.005 to 0.0085 and 0.0135 respectively. The equations were solved in transient mode. PISO algorithm was used for pressure velocity coupling while spatial discretisation scheme for vapour, energy and momentum were by second order upwind.

Figure 6 Grid independence study (see online version for colours)

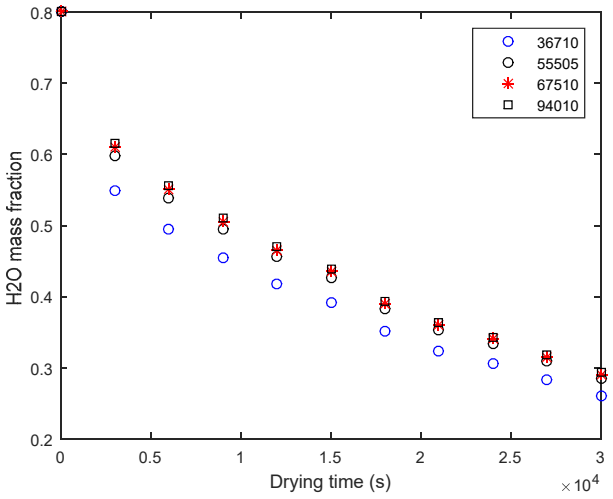

Table 6 Boundary condition at 313 K

Air temperature	*Location*	*Parameter*	*Symbol*	*Value*	*Units*
313 k	Inlet	Velocity	u	0.21	$m.s^{-1}$
				0.52	
				1^3	
		Specie mass fraction	H_2O	0.005	$kg.kg^{-1}$
			O_2	0.23	
	Fruit and drying air interface	Convective heat transfer coefficient	h_c	9.191	$w.m^{-2}$ K^{-1}
				14.282	
				17.823	
		Specie diffusive flux	H_2O	0.005	$kg.kg^{-1}$
			O_2	0.23	
	Drying air drier wall interface	Specie diffusive flux	H_2O	0	$kg.kg^{-1}$
			O_2	0	
	Drier wall	Specie diffusive flux	H_2O	0	$kg.kg^{-1}$
			O_2	0	
		Heat flux	q	0	$w.m^{-2}$

2.1 *Grid independence study*

Mesh with four different number of elements – 36710, 55505, 67510 and 94010 were used for the grid independence study. The changes in mass fraction of H_2O with respect to drying time for each of the element numbers were shown in Figure 6. The variation at 36710 elements compared to the rest was rather significant. Increasing the number of elements from 67510 to 94010 which was ≈28%

increase resulted into about 1% change in the value of H_2O mass fraction mid-way and towards the end of the drying period. Therefore for good accuracy and optimal computation time, a grid quantity of about 67510 was chosen for the simulations.

3 Results and discussion

3.1 Verification of the reliability of the code

The reliability of the code in predicting the drying behaviour of the chips was first verified using data from experiment conducted by Rosa (2016). The data were compared with those from the CFD setup and result (Figure 7) showed a reasonable agreement.

Figure 7 Comparing CFD result with data from experiment at 333 k (see online version for colours)

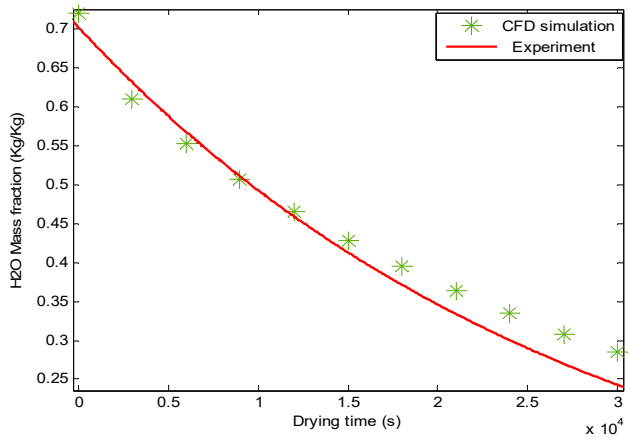

Figure 8 Velocity magnitude contour at 950 s and inlet velocity and of temperature 0.5 m/s and 323 k respectively (see online version for colours)

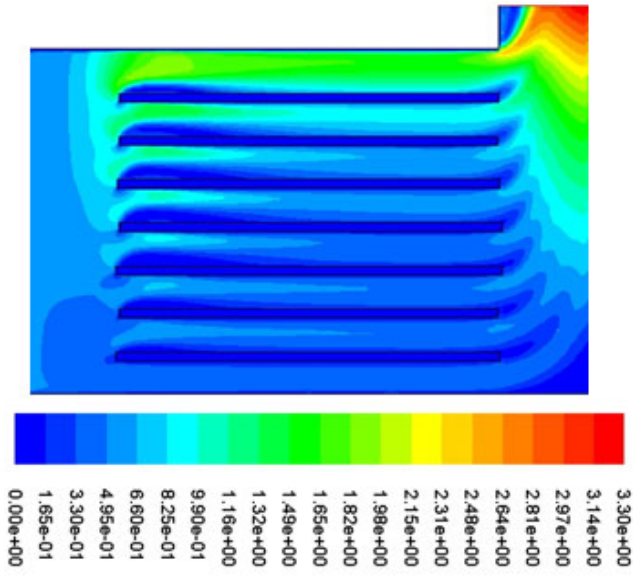

3.2 Overview of the CFD result

The velocity magnitude, mass fraction of H_2O and static temperature contours of the drier at 950 s, and air inlet temperature and velocity respectively of 323 K and 0.5 *m/s* are shown in Figures 6–10. The banana slices were fully exposed to the air stream (Figure 8). The humidity and temperature of drying air all over the chamber were uniform (Figure 9 and Figure 10).

Figure 9 H_2O mass fraction contour at 950 s and inlet velocity and of temperature 0.5 m/s and 323 k respectively (see online version for colours)

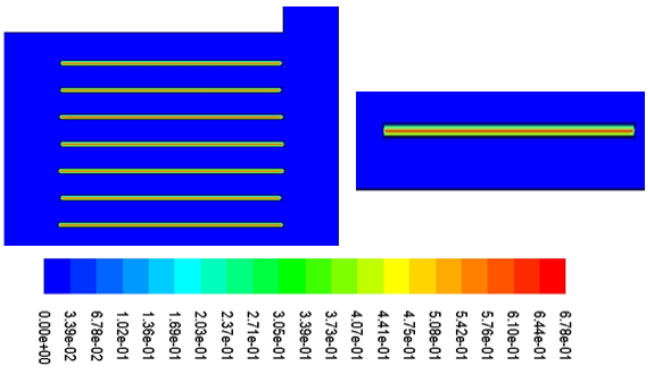

Figure 10 Static temperature contour at 950 s and inlet velocity and of temperature 0.5 m/s and 323 k respectively (see online version for colours)

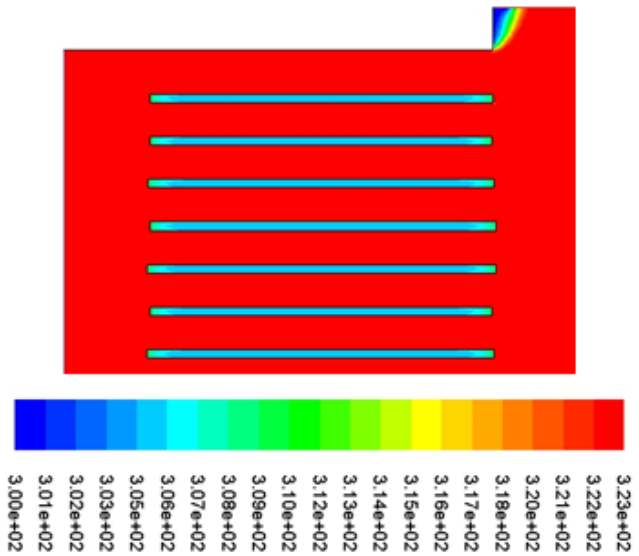

3.3 Velocity

Mass and convective heat transfer coefficients increased with velocity (equation (23) and Table 4). Velocity was responsible for keeping the drying space unsaturated because it affects the rate at which the evaporated/free species at the surface of the chips or regions close to it are transported to the environment . Varying the velocity impacts mainly on the transport of free species. It had no direct impact on the movement of species in the fruits interior due to resistance to flow arising from its compact structure.

3.4 Temperature

Drying rate increased significantly with temperature and showed only falling rate period (Figure 11). H_2O molecules at the surface became more agitated and broke loose from the surface and evaporate as temperature increased. This resulted in diffusion from the interior to the surface because of concentration gradient. As with all products that shows only falling rate period, the transport of species is dominated by diffusion which is measured by mass diffusivity or diffusion coefficient. This therefore is the major determinant of drying behaviour of the fruit and it increased with temperature.

Figure 11 Effect of temperature on drying curve (see online version for colours)

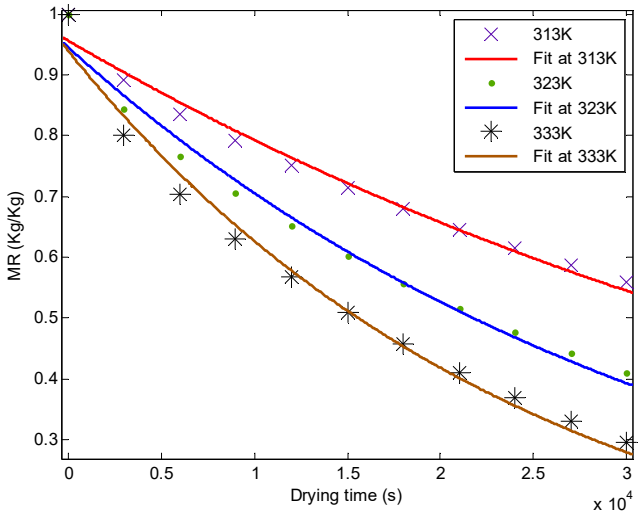

Figure 12 Volume ratio versus moisture content of banana at different temperatures (see online version for colours)

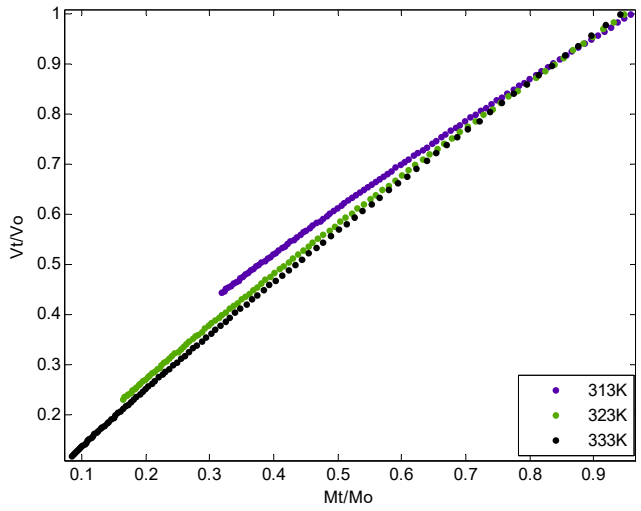

3.5 Shrinkage

In Figure 9, a substantial amount of water at the surface of the sample have been removed while those in the inner cells are relatively intact. This moisture removal gave rise to contraction that lead to shrinkage or reduction in volume. The deformation of cell walls due to shrinkage affects the diffusion process. This phenomena was factored into the drying model for more accurate determination of the effective diffusion coefficient. A plot of volume ratio and shrinkage coefficient against moisture ratio respectively were shown in Figure 12 and Figure 13. The curves are significantly influenced by temperature and approximately linear. Therefore, shrinkage is directly proportional to the volume moisture removed. Similar result were obtained by Guohong et al. (2012) and Mayor and Sereno (2004) for carrots and Amira et al. (2014) for cladode.

Figure 13 Shrinkage versus moisture content of banana at different temperature (see online version for colours)

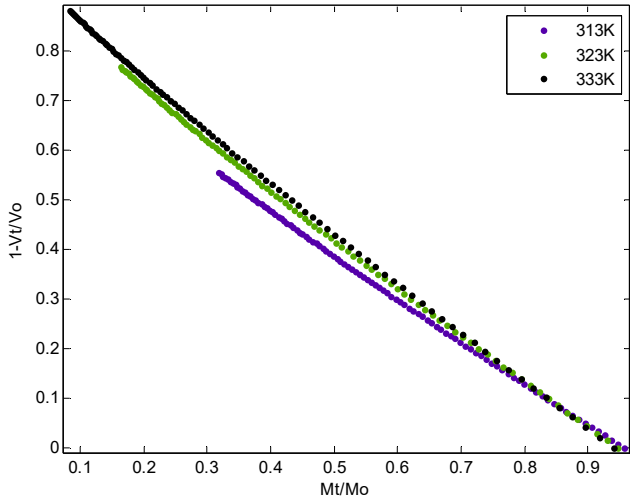

Figure 14 Variation of logarithm of moisture diffusivity with (1/T) for models that considered shrinkage and that that did not consider shrinkage (see online version for colours)

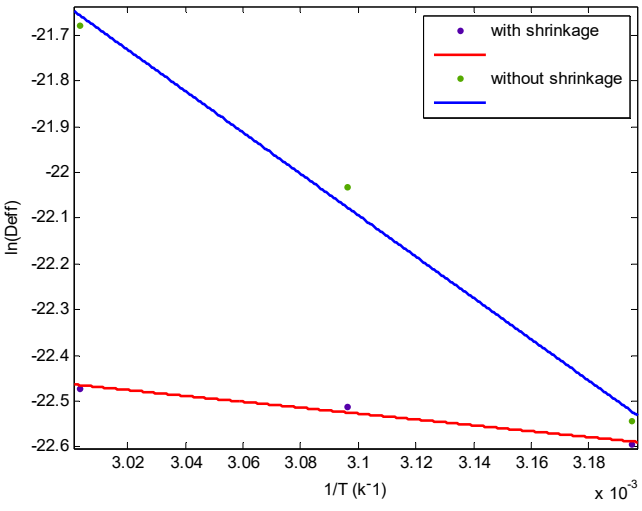

Table 7 Parameters and statistical indicators of Handerson and Pabis fit

TEMP	*a*	*k*	*Without shrinkage*	*With shrinkage*	R^2	*RMSE*	*SSE*
			D_{eff} (m^2 s^{-1})	D_{efs} (m^2 s^{-1})			
313K	0.9572	–1.877E-05	1.62E-10	1.54E-10	0.9829	0.01883	0.003190
323K	0.9463	–2.929E-05	2.71E-10	1.67E-10	0.9842	0.02420	0.005273
333K	0.9404	-4.049E-05	3.85E-10	1.74E-10	0.9850	0.02803	0.007069

3.6 Effective diffusivity

The drying curves (Figure 11) fits best with Handerson and Pabis model (Table 1). The fit parameters- shape factor (a), drying constant (k) and the statistical indicators (R^2, *RMSE* and *SSE*) are shown in Table 7. The effective diffusivities of the chips at test temperatures considering shrinkage and without shrinkage (D_{efs} and D_{eff}) in Table 7 were computed by comparing the fitted models to equation (8) and equation (7) respectively.

3.7 Activation energy

Arrhenius law equation (10) relates diffusion coefficient to temperature. From equation (10), the Plot of ln(D_{eff}) against $\frac{1}{T}$ is a straight line graph (Figure 14). The activation energy E_a computed from the slope and the pre-exponential factor D_O computed from the intercept were shown in Table 8 for model that factored in shrinkage and that without shrinkage.

Table 8 Parameters of effective diffusivity considering shrinkage and without shrinkage

Description	D_o (m^2 s^{-1})	E_a *(kJ/(mol)*	R^2
Considering shrinkage	1.213E-09	5.345	0.9736
Without shrinkage	3.1E-04	37.582	0.9853

4 Conclusions

The kinetics of thin layer drying of fruits has been studied numerically using unripe banana as sample. The computations were carried out to determine the impact of inlet air velocity and temperature on drying behaviour of fruits.

Transport of species from the fruits interior to the surface showed only falling rate period and therefore was dominated by diffusion which increased with temperature.

Velocity was responsible for bulk transport of evaporated H_2O at or close to the surface of the fruit to the environment. Increasing velocity impacts mainly on the transport of free species. It had little impact on species contained in the fruits interior due to resistance to flow arising from its compact structure.

The simulated drying curves fitted best with Handerson and Pabis model. The model was compared to two variants of Cranks solution for slab geometry. One modified to include shrinkage parameter and the other without modification. The result showed that effective diffusivity computed without considering shrinkage lead to overestimation of the parameter.

References

Amira, T., Saber, C. and Fethi, Z. (2014) 'Moisture diffusivity and shrikage of fruit and cladode of opuntia Ficus-Indica during infrared drying', *Journal of Food Processing*, Vol. 2014, pp.1–9, Article ID 175402.

Bohojlo-Wisniekwska, A. (2015) 'Numerical modelling of humid air flow around a porous body', *Acta Mechanica et Automatica*, Vol. 11, No. 3, pp.161–166.

Camelia, G., Adrian, G.G. and Ion, G. (2008) 'Heat and mass tranfer in convective drying processes', *Hanover*, *S.N.*, pp.1–4.

Clapp, J. (2015) *Food Self-sufficiency and International Trade: A False Dichotomy*, Food and Agricultural Organisation of the United Nations, Rome.

Daniel, E.C. et al. (2014) 'Mathematical Modelling and thermodynamic properties for drying soybeans grains', *African Journal of Agricultural Research*, Vol. 10, No. 1, pp.31–38.

Derossi, A., Severini, C. and Cassi, D. (2011) 'Mass tranfer mechanisms during dehydration of vegetable food: traditional and innovative approach', *InTech*, pp.305–354.

Guohong, L., Junruo, C., Meihong, L. and Xinxin, W. (2012) 'Shrinkage, porosity and density behaviour during convective drying of bio-porous material', *Pocedia Engineering*, Vol. 31, No. 2012, pp.634–640.

Incropera, F.P., Dewitt, D.P., Bergman, T.L. and Lavine, A.S. (2007) *Fundamentals of Heat And Mass Transfer*, 6th ed., John Wiley and Sons, Hoboken.

Iyang, U.E. and Oboh, I.O. (2018) 'Kinetic models for drying techniques-food materials', *Advances in Chemical Engineering and Science*, Vol. 2018, No. 8, pp.27–48.

Jaruk, S. and Roberts, J.S. (2007) 'Moisture transfer in solid food material: a review of mechanisms, models and measurement', *International Journal of Food Properties*, Vol. 2007, No. 10, pp.739–777.

Kenneth, J. and Hellevang, P. (1995) *Grain Moisture Content Effects and Mangement*, NDSU Extension Services, North Dakota.

Kumar, C., Karim, A., Joardder, M.U. and Miller, G.J. (2012) *Modelling Heat and Mass Transfer Process During Convection Drying of Fruit*, pp.1–8, ICCM, Gold Coast.

Lopez, R. et al. (2015) 'Heat and mass transfer analysis of convective drying of chickpea (Cicer Arietinum)', *Journal of Physics: Conference Series*, Vol. 2015, No. 582, pp.1–6.

Lutovska, M. et al. (2015) 'Modeling of thin layer drying of quince', *Journal of Processig and Energy in Agriculture*, Vol. 21, No. 2015, pp.12–16.

Mayor, L. and Sereno, A.M. (2004) 'Modelling shrinkage during convective drying of food materials: a review', *Journal of Food Engineering*, Vol. 69, No. 2004, pp.373–386.

Miroslawa, K., Kamil, S., Jerzy, G. and Dariusz, B. (2016) *Numerical Modelling of Heat and Mass Transfer in Vegetables Cold Storage*, pp.279–284, Elsivier, S.L.

Onwude, D.I. et al. (2016) 'Modelling the thin-layer drying of fruits anf vegetables: a review', *Comprehensive Reviews in Food Science and Food Safety*, Vol. 15, No. 2016, pp.599–619.

Rajasekar, S., Meyyappan, N. and Rao, D.G. (2016) 'A review on computational fluid dynamics studies in drying process', *Journal of Food Science Research*, Vol. 1, No. 1, pp.27–31.

Ramallo, L.A. and Mascheroni, R.H. (2011) 'Effect of shrinkage on prediction accuracy of the water diffusion model of pineapple drying', *Journal of Food Process Engineering*, Vol. 36, No. 2013, pp.66–76.

Roland, S. and Chaouat, B. (2022) 'Turbulence modeling and Simulation advances in CFD during the past 50 years', *Comptes Rendus Mecanique*, Vol. 2022, No. 350, pp.1–29.

Rosa, F.Z. (2016) *Mathmatical Modeling of Drying Process of Unripe Banana*, University of Sao Paulo, Sao Paulo.

Sabarez, H.T. (1998) *Chemical and Physical Changes During Dehydration of Prunes*, Doctor of Philosophy Thesis, Department of Chemistry.

Versteeg, H.K. and Malalasekera, W. (1995) *An introduction to Computational Fluid Dynamics an Introduction*, Longman Scientific and Technical, New York.

Zabski, J. (2015) 'Implemetation of first period of convective drying in a commercially available CFD package', *Transaction of the Institute of Fluid Flow Machinery*, Vol. 2015, No. 128, pp.139–157.